International Journal of Nanomedicine

Dovepress
open access to scientific and medical research

Open Access Full Text Article

ORIGINAL RESEARCH

Immunoliposome co-delivery of bufalin and anti-CD40 antibody adjuvant induces synergetic therapeutic efficacy against melanoma

This article was published in the following Dove Press journal:
International Journal of Nanomedicine
4 December 2014
Number of times this article has been viewed

Ying Li[1,*]
Jiani Yuan[1,*]
Qian Yang[1]
Wei Cao[1]
Xuanxuan Zhou[1]
Yanhua Xie[1]
Honghai Tu[2]
Ya Zhang[1]
Siwang Wang[1]

[1]Department of Natural Medicine and Institute of Materia Medica, School of Pharmacy, Fourth Military Medical University, Xi'an, People's Republic of China; [2]Institute for Drug and Instrument Control, Xinjiang Military Area Command, Urumqi, Xinjiang, People's Republic of China

*These authors contributed equally to this work

Abstract: Liposomes constitute one of the most popular nanocarriers for improving the delivery and efficacy of agents in cancer patients. The purpose of this study was to design and evaluate immunoliposome co-delivery of bufalin and anti-CD40 to induce synergetic therapeutic efficacy while eliminating systemic side effects. Bufalin liposomes (BFL) conjugated with anti-CD40 antibody (anti-CD40-BFL) showed enhanced cytotoxicity compared with bufalin alone. In a mouse B16 melanoma model, intravenous injection of anti-CD40-BFL achieved smaller tumor volume than did treatment with BFL (average: 117 mm^3 versus 270 mm^3, respectively); the enhanced therapeutic efficacy through a caspase-dependent pathway induced apoptosis, which was confirmed using terminal deoxynucleotidyl transferase-mediated dUTP-Fluorescein nick end labeling and Western blot assay. Meanwhile, anti-CD40-BFL elicited unapparent body-weight changes and a significant reduction in serum levels of tumor necrosis factor-α, interleukin-1β, interleukin-6, interferon-γ, and hepatic enzyme alanine transaminase, suggesting minimized systemic side effects. This may be attributed to the mechanism by which liposomes are retained within the tumor site for an extended period of time, which is supported by the following biodistribution and flow cytometric analyses. Taken together, the results demonstrated a highly promising strategy for liposomal vehicle transport of anti-CD40 plus bufalin that can be used to enhance antitumor effects via synergetic systemic immunity while blocking systemic toxicity.

Keywords: liposomes, bufalin, anti-CD40, chemoimmunotherapy

Introduction

Bufalin, one of the major digoxin-like components, is extracted from the skin and parotid venom glands of the toad *Bufo bufo gargarizans cantor* or *Bufo melanostictus*. Bufalin has excellent antitumor effects against various solid tumors, including those associated with leukemia, osteosarcoma, gastric cancer, prostate cancer, ovarian cancer, and colon cancer.[1–11] Previous studies have suggested that the anticancer activity of bufalin could be attributed to its well-documented inhibition of cell proliferation, induction of apoptosis, disruption of the cell cycle, and regulation of the immune response.[12,13] Although these results are promising, the use of this single chemotherapeutic drug is far from perfected and is associated with undesirable severe side effects such as immunosuppression, damage to normal tissues, high toxicity, and development of drug resistance.[14]

Tumors are known to elicit tolerated immune responses against tumor-associated self-antigens while simultaneously inducing local immune suppression as a mechanism to avoid detection and elimination by the host immune system itself. To some extent, these effects can be complemented and counterbalanced by immunotherapy. The overall goal of immunotherapy is the induction and amplification of functional

Correspondence: Wei Cao
Department of Natural Medicine and Institute of Materia Medica, School of Pharmacy, Fourth Military Medical University, 169 West Changle Road, Xi'an, 710032, People's Republic of China
Tel +86 29 8477 3752
Fax +86 29 8322 4790
Email caowei@fmmu.edu.cn

Si-Wang Wang
Department of Natural Medicine and Institute of Materia Medica, School of Pharmacy, Fourth Military Medical University, 169 West Changle Road, Xi'an, 710032, People's Republic of China
Tel +86 29 8477 4748
Fax +86 29 8322 4790
Email wangsiw@fmmu.edu.cn

antigen-specific immune responses for the development of long-lasting immunological memory to treat cancer. Immunotherapy is a novel treatment modality that kills tumor cells via induction of effective humoral immune responses. Intermediates of melanogenesis, which are simultaneously released by melanocytes, may even affect the immune system, and the response rates and low toxicities reported in malignant melanoma suggest that antigen-based active immunotherapy may complement current treatment, even though no relevant cancer vaccines for melanoma have been approved by the US Food and Drug Administration (FDA).[15–17] The major challenge to be solved is how to prevent melanoma from establishing neuroendocrine axes and rewiring the local and systemic homeostatic responses, in turn securing tumor survival and growth to the detriment of the host during stage 3 (regional metastasis) and stage 4 (diatal metastasis) disease.[18] For this reason, immunotherapy is emerging as a therapy in which the ability of the systemic immune system is exploited. The key to successful synergy therapy is to design a simple, novel co-delivery system that combines chemotherapy with immunotherapy in order to treat cancer patients while keeping side effects to a minimum.[19]

The various forms of combined immunotherapy include monoclonal antibodies (mAbs), adoptive lymphocyte transfer, and active specific immunotherapy, with monoclonal antibody therapy as the most common.[20,21] CD40 is a member of the tumor necrosis factor (TNF) receptor superfamily and is expressed on the surface of a variety of noncancer cells, such as B cells, macrophages, dendritic cells (DCs), myeloid cells, epithelial cells, and endothelial cells.[22,23] The CD40–CD40 ligand interaction provides a costimulatory signal to antigen-presenting cells (APCs), thereby augmenting the capability of APCs to present antigens and stimulating the production of proinflammatory cytokines and delivery-positive costimulatory signals, which in turn promotes antitumor cytotoxic T-cell responses. Qu et al[24] demonstrated that chemotherapy regimens with gemcitabine or 5-fluorouracil enhance the antitumor effect of anti-CD40 in the mouse B16 melanoma model. However, intravenous infusion of anti-CD40 mAbs results in inflammatory effects, such as symptoms of cytokine-release syndrome and liver damage due to systemic exposure.[25]

In light of the dangers of the potential systemic side effects, incorporating both a chemotherapeutic agent and monoclonal antibody delivery into the tumor sites simultaneously has been proposed to achieve a synergy for cancer therapies. Among several nanocarriers, including micelles, liposomes, and inorganic nanoparticles, liposomes have been extensively studied and are FDA-approved as a safe material for drug-delivery applications due to their enhanced permeability and retention mechanism (EPR effects).[26] Until now, most investigations demonstrated that liposomes are able to retain the bioactivity of therapeutics within local tumor tissues as well as improve the solubility of chemotherapy drugs. Li et al[27] prepared bufadienolides-loaded nanostructured lipid carriers, which showed an improved pharmacokinetic profile and reduced distribution in heart tissue. In this regard, polyethylene glycol (PEG) inserted into liposomes (PEGylated liposomes) are ideally suited because of their well-established versatile platform for exploring multiple approaches that not only potentially improved the delivery but also enhanced the local retention of therapies to the tumor itself.

In the present study, we employed a liposome co-delivery system that coupled anti-CD40 mAbs to the surface of PEGylated unilamellar liposomes wrapped with bufalin. This vector has shown a dual advantage of retaining the cytotoxic behavior of bufalin while expressing the immune response of anti-CD40. The combination chemoimmunotherapy of anti-CD40 plus bufalin by liposomal carriers was exploited to enhance anticancer therapeutic efficacy while reducing systemic toxicity, due to the confined biodistribution and prolonged release of cargo.

Materials and methods

Chemicals and reagents

L-α-phosphatidylcholine (EPC), cholesterol, dithiothreitol (DTT), and Tween 20 were purchased from Sigma-Aldrich (St Louis, MO, USA). 1,2-distearoyl-sn-glycero-3-phosphoethanolamine-N-[maleimide (polyethylene glycol)-2000] (DSPE-PEG_{2000}-Mal), 1,2-distearoyl-sn-glycero-3-phosphoethanolamine-N-[methoxy (polyethylene glycol)-2000] (ammonium salt; DSPE-PEG_{2000}), and rhodamine-phosphoethanolamine (Rho-PE) were obtained from Avanti Polar Lipids, Inc. (Alabaster, AL, USA). Bufalin (purity >98%) was purchased from BaoJi Chen-Guang Technology Development Co. Ltd (BaoJi, Shaanxi, People's Republic of China). Monoclonal anti-CD40 (clone FGK4.5, rat IgG2a) was purchased from Bio X Cell (West Lebanon, NH, USA). Zeba desalting columns were obtained from Pierce (Thermo Fisher Scientific, Rockford, IL, USA). Secondary antirat IgG was purchased from Jackson ImmunoResearch Labs (West Grove, PA, USA). Anti-CD40 enzyme-linked immunosorbent assay (ELISA) kits were purchased from Blue Gene Technology Development Co. Ltd (Shanghai, People's Republic of China). Antimouse CD45

(clone 30-F11), antimouse CD4, antimouse CD3, antimouse CD8a, and antimouse CD11c (N418) were obtained from Biolegend (San Diego, CA, USA). Cytochrome c and caspase-9 were obtained from Santa Cruz Biotechnology Co., Ltd (Dallas, TX, USA), and caspase-3 was obtained from ABclonal Biotech Co., Ltd (Cambridge, MA, USA).

Animals and cells

The animal experiments were conducted according to the Guidelines for Animal Experimentation of the Fourth Military Medical University (FMMU), Xi'an, People's Republic of China. The study protocol was approved by ethical committees of FMMU. C57/BL6 female mice were obtained from the Experimental Animal Center of FMMU at 6–8 weeks of age (initially weighing 20±2 g). Animal procedures were performed in accordance with the FMMU Institutional Authority for Laboratory Animal Care.

B16 melanoma cells (American Type Culture Collection CRL-6475™) were purchased from the FMMU Experimental Animal Center, cultured in Roswell Park Memorial Institute 1640 medium supplemented with 10% (v/v) fetal bovine serum and 1% antibiotics (100 U/mL penicillin G and 0.1 mg/mL streptomycin). Cells were maintained in their exponential growth phase in an atmosphere of 5% CO_2 and 90% relative humidity at 37°C.

Synthesis of bufalin liposome-anchored anti-CD40

Liposomes were prepared by thin lipid film hydration followed by sonication and extrusion as reported by Iyer et al.[28] In brief, liposomes were synthesized with a composition of cholesterol, EPC, DSPE-PEG_{2000}, DSPE-PEG_{2000}-Mal, and bufalin in a molar ratio of 20:55:5:5:15, respectively. Different ratios of phospholipid mixtures in chloroform were evaporated by a rotary evaporator at 35°C for 1 hour. The thin lipid layer was subsequently dried in a vacuum desiccator overnight to remove residual solvent (if any), and then the prepared dry thin film was rehydrated in phosphate-buffered saline (PBS) at 10 mmol/mL phospholipid at 60°C for 30 minutes to form maleimide-functionalized bufalin liposomes.

For preparation of bufalin liposome-anchored anti-CD40, anti-CD40 monoclonal antibody was conjugated to maleimide-functionalized liposomes through the maleimide–thiol reaction. In brief, anti-CD40 was mixed with excess DTT in the presence of 10 mM ethylene diamine tetraacetic acid (EDTA) in PBS for 20 minutes at 25°C and passed through a desalting column to remove unreacted DTT. The exposed sulfhydryl residues on the antibody were conjugated to maleimide-functionalized liposomes at a ratio of 1 mg antibody to 2 mmol liposomes for at least 10 hours at 25°C in the presence of 10 mM EDTA.

The resulting liposome suspension was immediately extruded with a LipoFast-Pneumatic Lipex extruder (Avestin; Ottawa, ON, Canada) five times using polycarbonate membranes (0.2 μm pore size; Whatman; Maidstone, UK) to form unilamellar liposomes, and then centrifuged and washed multiple times with PBS to remove unbound antibody and bufalin.

Characterization of liposomes

Particle size, zeta potential, and morphology of liposomes

The particle size distribution and zeta potential of liposomes were determined by dynamic light scattering technique using the Delsa™ Nano zeta potential analyzer (Beckman Coulter, Brea, CA, USA). Morphological evaluation of the liposomes was observed by a transmission electron microscope (TEM; Hitachi H-7650; Tokyo, Japan). For TEM studies, samples were placed over a copper grid and samples were negatively stained with 1% phosphotungstic acid.

Percentage entrapment of drugs in the liposomes

Percentage drug encapsulation in the liposomes was determined by centrifugation. The liposomes were centrifuged at 14,000 rpm for 20 minutes to remove the unloaded drug and then mixed with 10× volume of methanol to solubilize the lipids. The bufalin concentration was measured by high-performance liquid chromatography (HPLC). The entrapment efficiency of bufalin in the liposomes was estimated as:

$$E = (W_{encapsulated}/W_{total}) \times 100\%,$$

where E is the encapsulation efficiency of liposomes, $W_{encapsulated}$ is the measured amount of bufalin in the liposome suspensions after centrifugation, and W_{total} is the measured amount of bufalin in the equal volume of liposome suspensions before centrifugation.[29]

Bufalin was quantified by an Xtimate C18 column (250×4.6 mm, 5 μm) (Welch Materials, Inc., Shanghai, People's Republic of China) and detected by HPLC with a photodiode array detector method. The mobile phase was composed of 1) 0.5% monopotassium phosphate (adjusted to pH 3.2 using phosphoric acid) and 2) acetonitrile, using a gradient elution and performed at 40°C with a flow rate of 1.0 mL/minute.

In vitro release of bufalin and anti-CD40 from liposomes

The in vitro release behaviors of bufalin and anti-CD40 mAbs from the liposomes were investigated using dialysis. Briefly, 1 mL of liposomal solution was dialyzed against 20 mL PBS (pH 7.4) containing 10% fetal calf serum in a dialysis tube (molecular weight cutoff =30 kDa) with gentle horizontal shaking (120 rpm). The dialysate was withdrawn from the medium and replaced with an equal volume of fresh PBS at the predetermined time points. The concentration of bufalin was measured by HPLC, and anti-CD40 was measured by ELISA according to the manufacturer's protocol.

In vitro cell cytotoxicity

In vitro cytotoxicity was evaluated using the cholecystokinin (CCK)-8 assay (Beyotime Institute of Biotechnology, Shanghai, People's Republic of China). B16 cells were seeded in 96-well microtiter plates at a density of 5×10^4 cells per well and incubated (37°C, 5% CO_2) for 24 hours. Anti-CD40 solution, free bufalin, BFL, and anti-CD40-BFL were added to cells in a total final volume of 100 μL per well for 6 hours and 24 hours. The BFL and anti-CD40-BFL with bufalin concentrations of 500 μmol/L were prepared, and diluted into bufalin concentrations of 300 μmol/L, 250 μmol/L, 200 μmol/L, 150 μmol/L, 100 μmol/L, and 50 μmol/L consecutively. The concentrations of free antibody were identical to the concentrations of the antibody conjugated to liposomes, and the blank liposomes were evaluated to test the toxicity of the nanocarrier. Ten microlitres of CCK-8 assay agents were added to the culture medium at given time intervals, and the cells were incubated for another hour. Absorbance was measured on a microplate reader at 450 nm with a reference wavelength of 690 nm.

In vivo antitumor efficacy

For in vivo tumor experiments, approximately 5×10^4 B16 cells suspended in physiological saline were subcutaneously injected into the hind flank of female C57/BL6 mice on day 0. After the growing tumors were palpated, mice were assigned randomly into five groups (eight mice per group). Tumor sizes were measured by vernier caliper and calculated using the following equation: volume (mm^3) = (major axis × minor axis^2) ×0.5. The antitumor therapy experiments were commenced when tumor size reached 3–5 mm in diameter on day 9. The mice were then treated with tail-vein injections of PBS, bufalin solution, soluble anti-CD40, BFL, or anti-CD40-BFL from day 9–15 every other day. The bufalin dose was 1 mg/kg and the anti-CD40 dose was 8 mg/kg in each pure or liposome solution. Throughout the study, weight and tumor size were monitored daily. Mice were sacrificed when the tumor size in the control group reached 800 mm^3, and every tumor, spleen, and lymph node were harvested. One portion of the harvested tumors was fixed in 10% formalin, processed into paraffin-embedded sections at a thickness of 4 μm, and stained with hematoxylin and eosin for histopathological analysis.

Serum measurements of serum cytokine levels

For the measurement of circulating inflammatory markers, serum samples were taken via retro-orbital bleeding after injection for 24 hours, followed by centrifugation at 5,000 rpm to remove the cellular fraction. Circulating serum levels of TNF-α, interleukin (IL)-1β, IL-6, and interferon (IFN)-γ were quantified by ELISA according to the manufacturer's protocol. The serum level of free anti-CD40 was measured by ELISA using recombinant CD40 receptor. Levels of the hepatic enzyme alanine transaminase (ALT) were measured using a standard biochemical assay (Infinity ALT reagent kit; Thermo Fisher Scientific).

Apoptosis assay

Tumors were isolated and immediately snap-frozen and sliced at a thickness of 10 μm during cryosectioning. The cryosections were mounted onto Superfrost Plus glass slides (Fisher Scientific; Houston, TX, USA) and fixed with acetone. The cell apoptosis of tumors was confirmed by in situ fluorescent terminal deoxynucleotidyl transferase-mediated dUTP-Fluorescein nick end labeling (TUNEL) staining, according to the manufacturer's protocol (Roche, Basel, Switzerland). Briefly, the cryosections were fixed by 4% paraformaldehyde in PBS for 20 minutes and then permeabilized on ice and incubated with the TUNEL reaction mixture at 37°C for 1 hour. The fluorescein labels incorporated into the damaged sites of the DNA were detected by fluorescent microscopy. Subsequently, the slides were treated with 50 μL 4,6-diamidino-2-phenylindole solution (5 μg/mL) for 10 minutes to stain the nuclei, washed thrice, and covered by antifade mounting medium. Images were taken under a FluoView FV1000 confocal microscope (Olympus, Tokyo, Japan).

Western blot analysis

Frozen tissue samples (~100 mg) were quickly homogenized in lysis buffer (1% Triton ×-100, 50 mM Tris HCl, 150 mM

NaCl) containing protease inhibitors. After 30 minutes incubation on ice, samples were centrifuged for 30 minutes at 4°C at 14,000 rpm. The supernatants were assayed for protein levels according to the Bradford method with bovine serum albumin as the standard. Aliquots of 50 μg of protein in each sample were denatured at 90°C for 5 minutes, resolved by 12% sodium dodecyl sulfate polyacrylamide gel electrophoresis, and then transferred onto a polyvinylidene difluoride membrane. The blotted membrane was blocked with 5% nonfat milk in PBS pH 7.4 plus Tween 20 and incubated with the respective primary antibodies (cytochrome c, caspase-3, caspase-9, or β-actin as a standard) at 4°C overnight, washed, and then incubated with the corresponding horseradish peroxidase-conjugated antimouse secondary antibody for 2 hours. After several washes, the immunoreactions were visualized by an enhanced chemilumescent detection kit (GE Healthcare Life Sciences, Piscataway, NJ, USA) and exposed to X-ray film. Films of Western blots were scanned and quantified using an image processor.

Immunofluorescence analysis of anti-CD40-BFL distribution and flow cytometric analysis

For analysis of the anti-CD40-BFL distribution, we prepared BFL and anti-cD40-BFL using 0.5 molar Rho-PE as fluorescence probe. After treatment with the Rho-PE liposomes, tumors, lymph nodes, and spleen were isolated, immediately snap-frozen using liquid nitrogen for cryosectioning, and sliced at a thickness of 10 μm. The cryosections were fixed by 4% paraformaldehyde in PBS for 20 minutes and then incubated with a DyLight448-labeled conjugated secondary antibody at a 1:200 dilution at 37°C for 30 minutes. Slides were washed and covered using antifade mounting medium, and images were taken under the confocal microscope.

The tumor, lymph nodes, and spleens were cut into pieces and digested with 0.25% trypsin for 10 minutes at 37°C, followed by filtration through a cell mesh to obtain cell suspensions. The cells were washed twice with PBS containing 1% bovine serum albumin, blocked using 10% fetal bovine serum, and stained with fluorescent antibodies against CD45, CD11c, CD3, CD4, and CD8a for 30 minutes at 37°C. After two washes with PBS, the cell suspensions were used for flow cytometery (Becton Dickinson, San Jose, CA, USA).

Statistical analysis

Data from each group are presented as the mean ± standard error of the mean. Statistical significance was evaluated using Student's *t*-test and a one-way analysis of variance followed by a posteriori testing with Dunnett correction, performed using Graphpad Prism 5.0. A *P*-value of <0.05 was considered statistically significant.

Results

Synthesis and characterization of anti-CD40-BFL

Liposomes combined with anti-CD40 mAbs restricted the dissemination of conjugated ligands and resulted in subdued systemic toxicity and side effects. mAbs binding to the maleimide-functionalized liposomes containing the mixture of cholesterol, EPC, DSPE-PEG_{2000}, DSPE-PEG_{2000}-Mal, and bufalin (20:55:5:5:15 molar ratio) is illustrated as a schematic in Figure 1A. The disulfides in the hinge region of the antibody mildly reacted with maleimide, and the amount of mAbs conjugated was only closely related to the quantity of maleimide–PEG–lipid and weakly influenced because the vesicle composition was settled. To evaluate the efficiency of our synthesis, the concentration of anti-CD40 was measured by ELISA analysis of liposomes lysed by Tween 20 surfactant, and anti-CD40 density on the liposomes was estimated to be 5 mg/mL.

The particle size distribution and zeta potential of liposomes, measured by dynamic light scattering, are summarized in Figure 1B. Anti-CD40-BFL had a mean particle size of approximately 205.4±68.4 nm with a narrow range of size distribution (polydispersion index =0.062), while the mean particle size of BFL was 171.4±69.2 nm (polydispersion index =0.088). All liposome formulations exhibited a similar negative surface charge, suggesting excellent stability (anti-CD40-BFL: −15.68 mV; BFL: −30.71 mV; Table S1). The surface morphology determined by TEM revealed a uniform spherical shape, and the sizes were smaller than those from dynamic light scattering due to the presence of hydrated layers around the particle surfaces (Figure 1C). However, the drug encapsulation efficiency of BFL and anti-CD40-BFL as determined by HPLC were 87.85%±4.23% and 73.59%±3.14%, respectively. Anti-CD40-BFL had a lower drug encapsulation efficiency, which was mainly due to the prolonged time it was stirred.

The cumulative drug release profiles of bufalin and anti-CD40 from liposomes in vitro indicated that free bufalin and anti-CD40 could be nearly 80% from solution within 4 hours, suggesting it diffused through the dialysis membrane freely (Figure 2). By contrast, the liposomes had a substantially good shelf life. As for anti-CD40-BFL, the initial release of bufalin began at 6 hours, indicating that bufalin was steadily

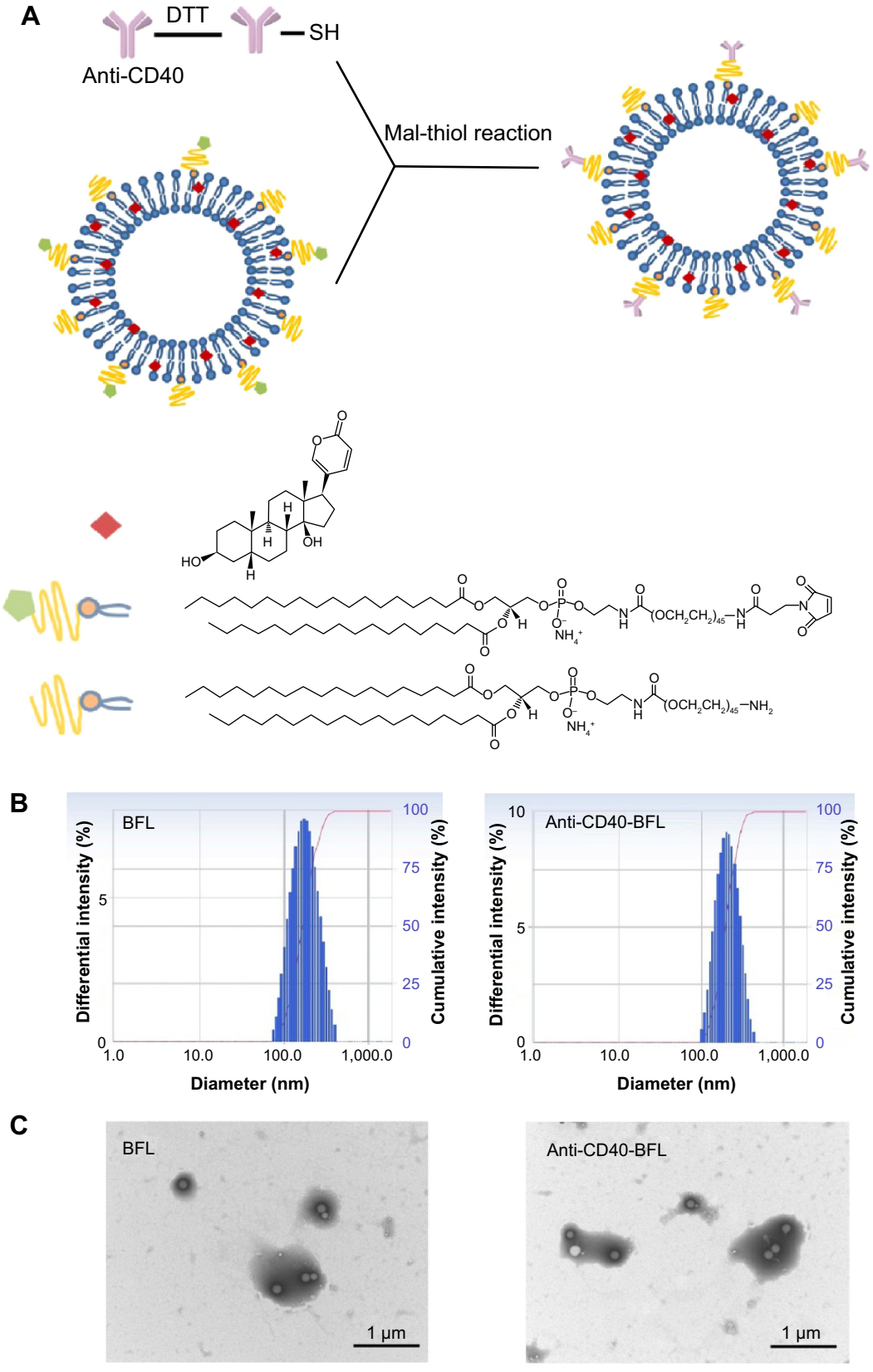

Figure 1 Preparation schematic and characterization of PEGylated liposomes containing bufalin with or without anti-CD40.

Notes: (**A**) Schematic illustration of the surface coupling of anti-CD40 to PEGylated liposomes via maleimide–thiol reaction. (**B**) Particle size distribution of BFL and conjugated with anti-CD40 antibody (anti-CD40-BFL) in the range of 150–200 nm, as measured by dynamic light scattering. (**C**) TEM images of BFL and anti-CD40-BFL, with a uniform spherical shape.

Abbreviations: BFL, bufalin liposomes; DTT, dithiothreitol; Mal-thiol, maleimide–thiol; SH, sulfhydryl; TEM, transmission electron microscope.

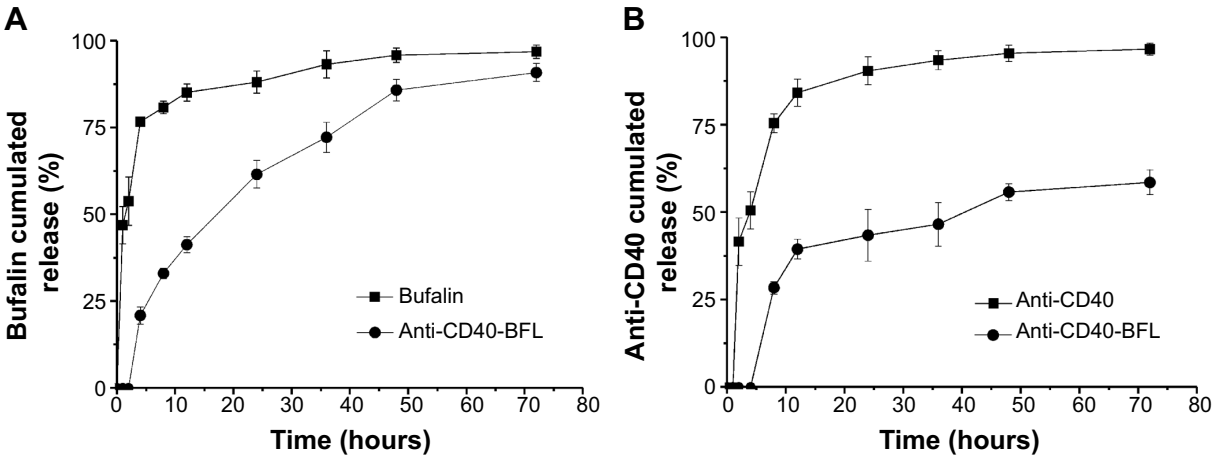

Figure 2 In vitro release profiles of bufalin and anti-CD40 from combination liposomes by dialysis against phosphate buffered saline, compared to the dialysis of freely soluble bufalin and anti-CD40.
Notes: The results are a representative of three independent experiments. (**A**) Release of encapsulated bufalin from combination liposomes was measured by high-performance liquid chromatography and occurred more slowly than release of freely soluble bufalin. (**B**) Release of conjugated anti-CD40 from combination liposomes was measured by enzyme-linked immunosorbent assay and reached a plateau after 2 days.
Abbreviation: BFL, bufalin liposomes.

incorporated into the lipid bilayer due to its semblable structure of cholesterol and no evidence of drug burst release. Approximately 90% of bufalin was released within 72 hours, while anti-CD40 was close to 50%. The release profiles obtained from both bufalin and anti-CD40 indicated that the co-delivery system provided a possibly synergistic effect.

In vitro cytotoxicity

The CCK-8 assay was carried out to determine the cell viability (Figure 3). Bufalin caused a dramatic inhibition of growth in B16 cells in a dose-dependent manner, while changes in cell viability of blank liposomes did not indicate any changes in cell viability. Cell viability was <50% after treatment with 300 nmol/L of free bufalin for 6 hours, which was significantly higher than that of liposomes, dominantly attributed to the controlled release of liposome. After 24 hours, the cell viability of bufalin was adverse, while BFL exhibited remarkable cytotoxicity on B16 cells, explained by the fact that cells could efficiently uptake liposomes through endocytosis, consistent with IC_{50} (median inhibition

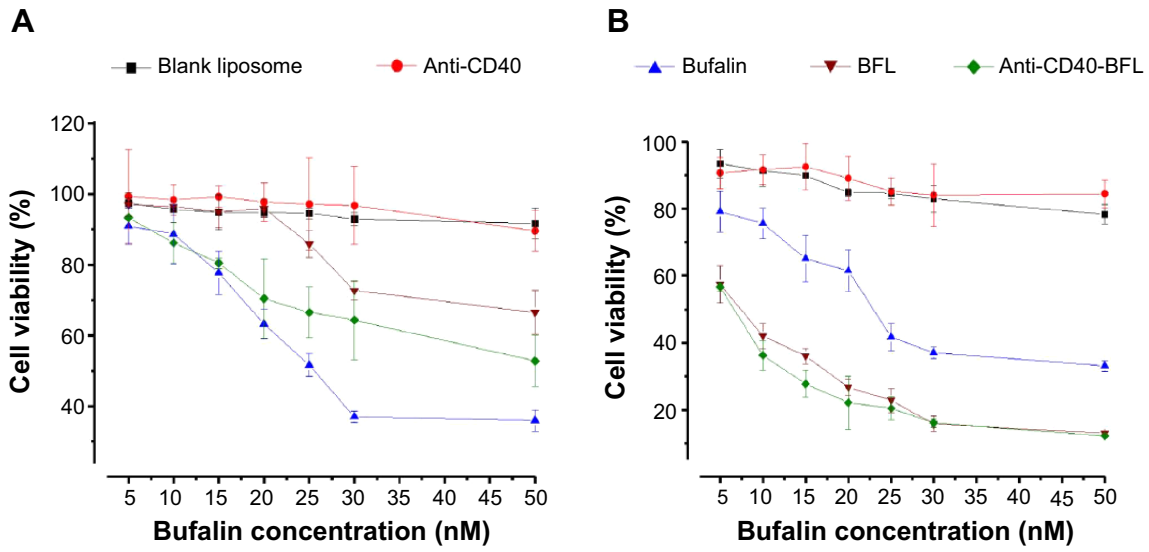

Figure 3 In vitro cytotoxicty of blank liposome, free anti-CD40, bufalin, BFL, and anti-CD40-BFL against B16 melanoma cells.
Notes: The diagrams of B16 melanoma cell viability at various drug concentrations (**A**) after 6 hours of treatment and (**B**) after 24 hours of treatment. Bufalin showed a higher cytotoxicity on B16 cells than liposomes after 6 hours, due to the controlled release of liposome. After 24 hours, the cell viability was adverse. The cell viabilities of BFL and anti-CD40-BFL were similar, attributable to the absence of CD40 surface expression on B16 cells. Data are presented as mean ± standard deviation (n=6).
Abbreviation: BFL, bufalin liposomes.

concentration) results (Table S2; other data not shown). However, the growth inhibitory effect between BFL and anti-CD40-BFL was similar, which can possibly be attributed to the anti-CD40 solution having little effect on cell viability, as previously observed by Kwong et al[25] due to the absence of CD40 surface expression on B16 cells.

In vivo therapeutic efficacy

We evaluated the therapeutic efficacy in C57/BL6 mice bearing B16 cell subcutaneous tumors. After the tumors were palpated (40 mm^3), physiological saline was administered via tail-vein injection into mice in the control group. Bufalin solution, anti-CD40 solution, BFL, and anti-CD40-BFL at an equivalent dosage of 1 mg/kg bufalin or 8 mg/kg anti-CD40 antibody per injection were administered by tail-vein injection in the treatment groups every other day, five times.[30] As illustrated in Figures 4A and C, tumor growth was significantly inhibited in all treatment groups compared with the control group (physiological saline). Anti-CD40-BFL showed greater tumor growth inhibition than bufalin solution alone, which is consistent with the cytotoxic effects observed in vitro, resulting in average tumor volumes of 176.34±43.86 mm^3 versus 284.35±84.05 mm^3, respectively (P=0.0341). Therapeutic efficacy was enhanced obviously between anti-CD40-BFL and BFL (average tumor volumes of 176.34±43.86 mm^3 versus 254.53±44.99 mm^3, P=0.0482), as the activated immune response pathways of anti-CD40 could overcome the immunosuppression present in advanced tumors and induce cytotoxic T lymphocyte responses. Nonetheless, the anti-CD40 solution group (average tumor volumes of 477.96±76.89 mm^3, P=0.0041) showed a limited therapeutic effect relative to anti-CD40-BFL, which can be attributed to the potent anticancer effect of bufalin. In addition, the average tumor weight in the physiological saline,

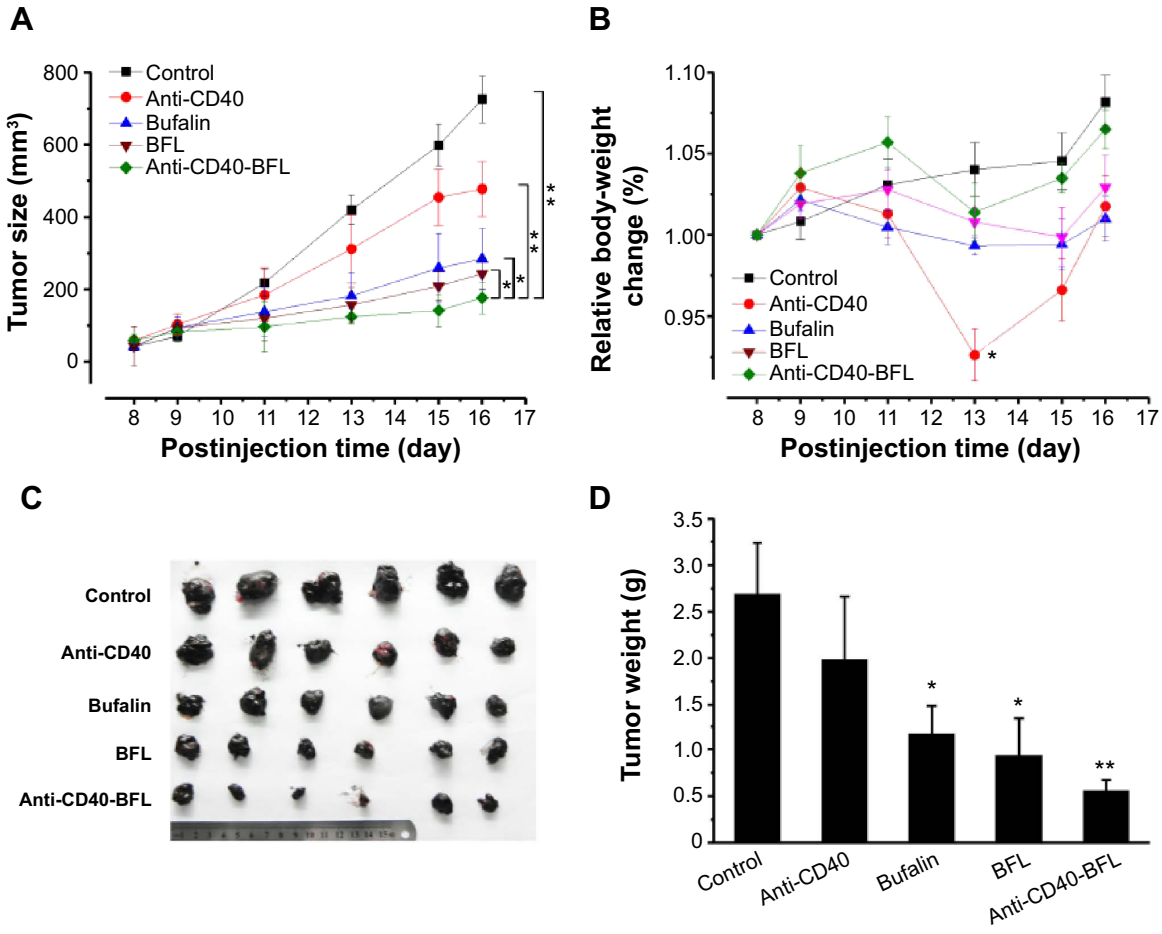

Figure 4 Therapeutic efficacy on C57/BL6 mice carrying subcutaneous B16 melanoma tumors.
Notes: (**A**) Average tumor growth curves from a representative experiment. Mice were given tail-vein injections on day 9, day 11, day 13, and day 15 following tumor cell inoculation with phosphate-buffered saline, soluble anti-CD40, bufalin, BFL, or anti-CD40-BFL at an equivalent dose of 1 mg/kg or 8 mg/kg of anti-CD40 per injection. (**B**) Body-weight changes of the mice over the experimental period. (**C**) Photographs of melanoma tumors in each group. (**D**) Average tumor weight at the endpoint of study. *P*-values were determined by paired Student's *t*-tests: *$P<0.05$, **$P<0.01$ (n=6, mean ± standard error).
Abbreviation: BFL, bufalin liposomes.

bufalin solution, anti-CD40 solution, BFL, and anti-CD40-BFL groups at the end of the experiment were 2.68 g, 1.97 g, 1.15 g, 0.93 g, and 0.55 g, respectively (Figure 4D), and the anti-CD40-BFL group had the lowest tumor weight among all the treatment groups (P=0.0303).

Average body weight changes were observed in order to estimate systemic toxicity (Figure 4B). The anti-CD40 group experienced substantial weight loss relative to the PBS control group, with a weight loss peak of about 8% after two injections. This could be attributed to the ability of anti-CD40 to enter into systemic circulation rapidly after injection to cause widespread inflammatory effects. To the contrary, the body-weight loss in the anti-CD40-BFL group was minimal, since the liposome-based antigen delivery system could provide prolonged and simultaneous delivery of antigen.

Liposome-triggered tumor cell apoptosis

Apoptotic signaling cascades result in single-stranded and double-stranded DNA fragmentation and can be detected by TUNEL assay using an in situ cell death detection kit. As shown in Figures 5A and C, the cytosections of the control group had no visible green fluorescence, suggesting the absence of cell apoptosis, while the mild fluorescence in the soluble anti-CD40 and bufalin groups demonstrated partial apoptosis of B16 cells. In contrast, anti-CD40-BFL exhibited stronger fluorescence in most of the cells, indicating an increase in apoptosis in vivo. In addition, hematoxylin and eosin histological analysis of paraffin sections confirmed apoptosis (Figure 5B).

In vivo apoptosis results were verified by Western blot analysis. To determine whether apoptosis is mediated via the activation of caspase-3, caspase-9, and cytochrome c, tumors were harvested and apoptosis-associated protein levels were quantified. As shown in Figure 5D, the integral optical density of anti-CD40-BFL was strongest in caspase-3 (0.92±0.026), caspase-9 (1.58±0.013), and cytochrome c (1.069±0.016), suggesting that anti-CD40-BFL elicits the most powerful apoptosis effect compared with other treatment groups, via a mitochondria-dependent pathway.

Serum cytokine levels

Serum cytokine levels administered 24 hours posttreatment were measured to evaluate systemic toxicity (Figure 6). Anti-CD40-BFL treatment resulted in significantly lower serum levels of TNF-α, IL-1β, IL-6, and IFN-γ compared with soluble anti-CD40 mAbs, indicating that the anchoring of anti-CD40 to the liposome could reduce systemic toxicity. The serum levels of TNF-α were 1.56±0.73 ng/L, 40.14±1.91 ng/L, 13.72±2.27 ng/L, 10.14±5.18 ng/L, and 24.3±0.76 ng/L for the physiological saline, anti-CD40 solution, bufalin solution, BFL, and anti-CD40-BFL groups, respectively. Similar trends were observed with IL-1β (2.54±1.07 ng/L, 40.14±1.91 ng/L, 13.89±2.21 ng/L, 16.28±2.76 ng/L, and 14.15±2.53 ng/L, respectively), IL-6 (1.99±0.96 ng/L, 28.07±2.19 ng/L, 6.86±2.64 ng/L, 7.37±1.48 ng/L, and 11.98±2.34 ng/L, respectively) and IFN-γ (13.81±4.92 ng/L, 776.90±37.82 ng/L, 487.23±98.62 ng/L, 332.86±75.95 ng/L, and 534.83±55.14 ng/L, respectively). The serum levels of ALT enzyme (0.709±0.065 ng mL, 5.872±0.146 ng/mL, 1.613±0.267 ng/mL, 1.808±0.445 ng mL, and 2.492±0.453 ng/mL, respectively) suggested that the liposome has low toxicity in the liver and that there were no significant safety issues.

Biodistribution of anti-CD40-BFL

In order to investigate the biodistribution of anti-CD40-BFL, immunofluorescence histological analysis on cryosections of tumors, spleens, and lymph nodes were performed to directly visualize the local retention of liposomes and anti-CD40. As illustrated in Figure 7, the red fluorescence of liposomes was retained at a high level within the tumor for 24–48 hours postinjection, while anti-CD40 (green) still remained coupled to the liposome (merged for yellow) in vivo. The liposome-anchored anti-CD40 could lead to sustained release and enhanced retention of anti-CD40 in the tumor area, which coincides with the delayed release properties of anti-CD40-BFL in vitro.[31] Meanwhile, the labeled liposomes could be found in spleens and lymph nodes after 48 hours, which implied liposome-induced immunity in both local and systemic immunotherapy. Green fluorescence was barely observed following soluble anti-CD40 therapy after 24 hours, indicating rapid entrance into systemic circulation, which indicates a huge hidden risk of cytokine-release syndrome and short curative effect.

CD40 plays a pivotal role in the immune response via interactions between T cells and antigen-presenting cells. Tumor tissues, spleens, and lymph nodes were harvested 24 hours or 48 hours postinjection and processed into cell suspensions for flow cytometer analysis. Figure 8 illustrates that the amount of DCs ($CD11c^+$, $CD45^+$), $CD4^+$ T cells ($CD3^+$, $CD4^+$), and $CD8^+$ T cells ($CD3^+$, $CD8a^+$) were positive for anti-CD40-BFL, suggesting the successful delivery of anti-CD40 to its intended targets. After injecting anti-CD40 solution for 24 hours, the quantities of $CD4^+$ T cells in tumor tissues, spleens, and lymph nodes were higher than in tissues injected with anti-CD40-BFL, and were mainly distributed in spleens and lymph nodes, and only a few in tumors. Forty-eight hours after injection, the number of $CD4^+$ T cells in all tissues was reduced, while

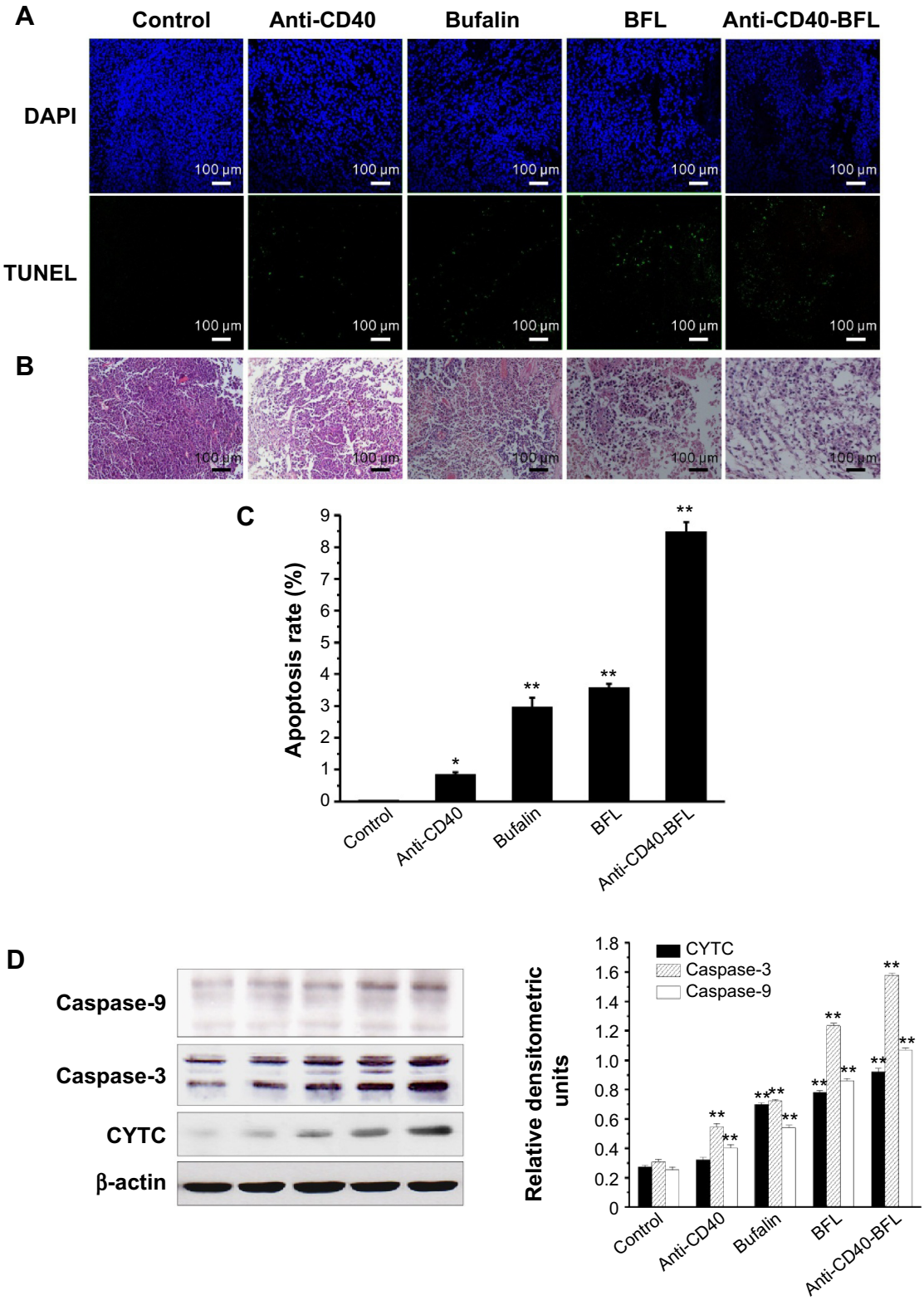

Figure 5 Apoptosis in control and tumor cells.

Notes: (**A**) Typical fluorescence microscopic images of TUNEL staining of tumor cytosections treated with saline, free anti-CD40, bufalin, BFL, or anti-CD40-BFL; scale bars denote 100 μm. Blue: cell nuclei, DAPI. Green: apoptosis cells. (**B**) H&E-stained tumor paraffin sections from mice at the endpoint of the study after treatment with saline, free anti-CD40, bufalin, BFL, or anti-CD40-BFL. Original magnification: 100×. (**C**) Histogram of mean apoptotic index in each group. (**D**) Western blot analysis of cytochrome c, caspase-3, and caspase-9 protein in tumor tissues after treatment with saline, free anti-CD40, bufalin, BFL, or anti-CD40-BFL. *P*-values were determined by paired Student's *t*-tests: *$P<0.05$, **$P<0.01$ (n=6, mean ± standard error).

Abbreviations: BFL, bufalin liposomes; CYTC, cytochrome c; DAPI, 4,6-diamidino-2-phenylindole; H&E, hematoxylin and eosin; TUNEL, terminal deoxynucleotidyl transferase-mediated dUTP-fluorescein nick end labeling.

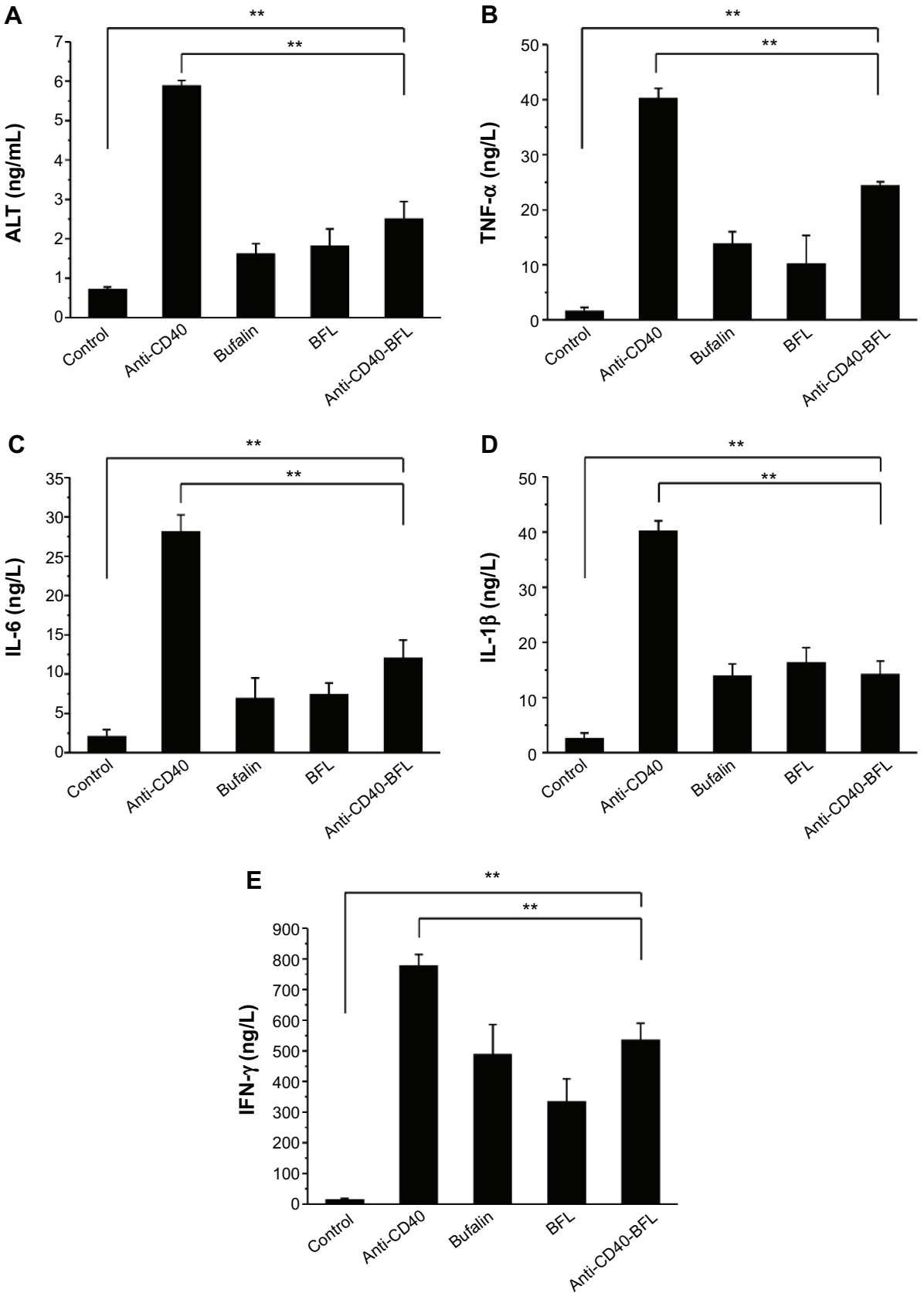

Figure 6 Serum circulating inflammatory marker levels.

Notes: Serum circulating levels 24 hours after the first dose of saline, free anti-CD40, bufalin, BFL, or anti-CD40-BFL. (**A**) Hepatic enzyme ALT. Inflammatory cytokines (**B**) TNF-α, (**C**) IL-6, (**D**) IL-1β, and (**E**) IFN-γ. *P*-values determined by unpaired Student's *t*-test: $^{**}P<0.01$.

Abbreviations: ALT, alanine transaminase; BFL, bufalin liposomes; IFN, interferon; IL, interleukin; TNF, tumor necrosis factor.

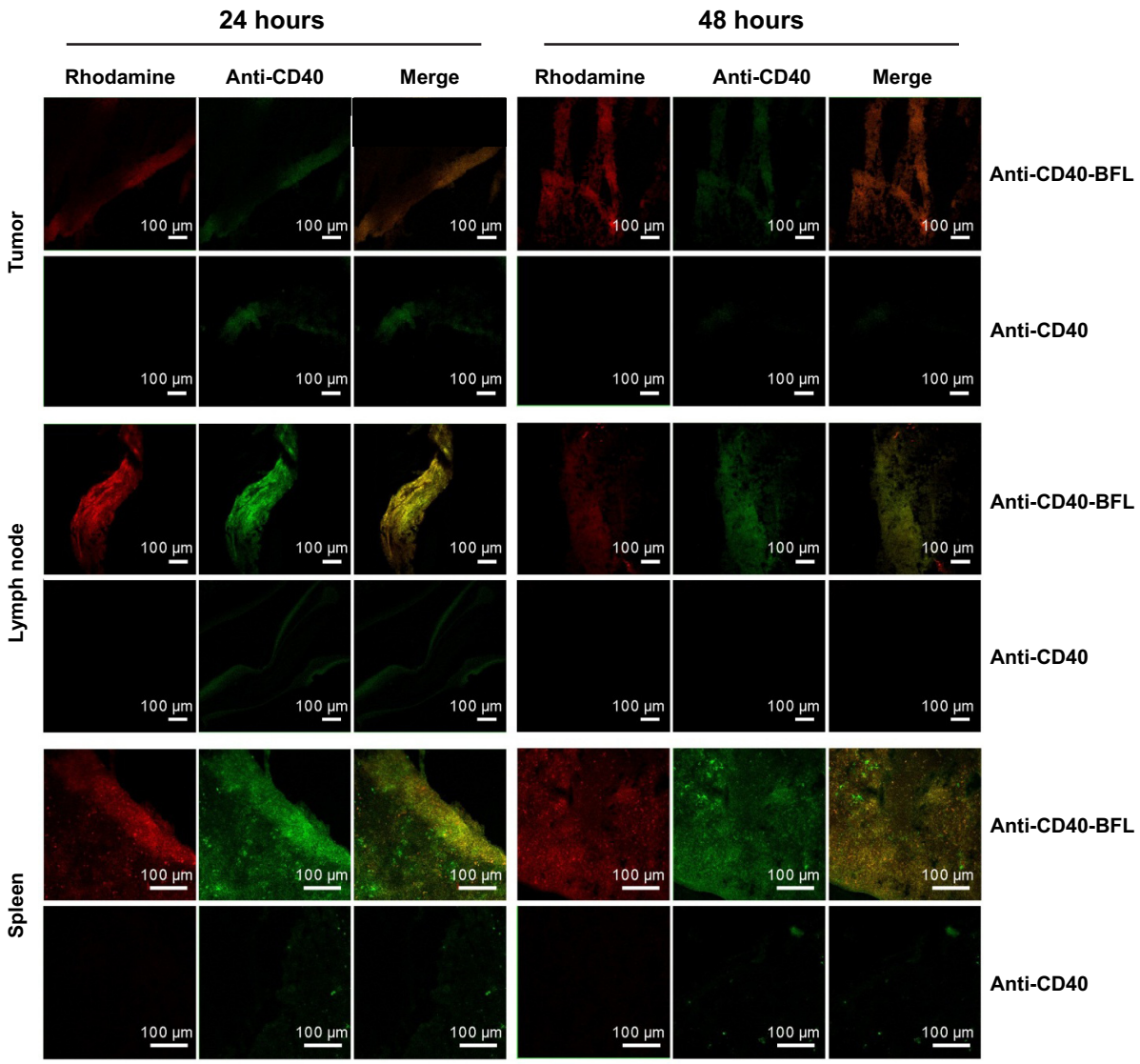

Figure 7 Immunofluorescence analysis of frozen tissue sections.
Notes: Immunofluorescence analysis of frozen tissue sections shows fluorescence rhodamine-labeled liposomes (red), anti-CD40 (green), and merged (yellow) images. Scale bars denote 100 μm. Liposomes were retained at a high level within the representative cryosections of tumors, spleens and lymph nodes for 24–48 hours postinjection, and anti-CD40 still remained coupled to the liposome in vivo. Meanwhile, green fluorescence was barely observed following an injection of soluble anti-CD40 therapy after 24 hours and nearly disappeared after 48 hours.
Abbreviation: BFL, bufalin liposomes.

the ratio in anti-CD40 solution and anti-CD40-BFL increased. In addition, the fewest $CD4^+$ T cells were found in the bufalin groups, suggesting an immunosuppressive effect. A similar result was found for DCs and $CD8^+$ T cells.

Discussion

We have successfully developed an anti-CD40 antibody-mediated bufalin liposome, which was utilized to stimulate apoptosis of B16 melanoma cells, delay growth of tumors, and eliminate systemic side effects (Figure 9). The liposomal delivery vehicle utilized, not only overcame the disadvantages of bufalin, which include poor solubility, immunosuppression, and damage to normal tissue, but also allowed for anti-CD40 to elicit synergistic antitumor effects.

Melanoma, an aggressive skin cancer, represents 4% of all dermatologic cancers yet accounts for more than 80% of all deaths from skin cancer, leaving patients with metastatic melanoma with a 5-year survival rate of <5%.[32] Although surgical management remains the primary modality of therapy for patients, it cannot clear tumorigenic or metastatic cells completely and requires supplementation by chemotherapy and/or radiotherapy.[33,34] Treatment options for these patients are limited, and no specific immunotherapy vaccine has been approved by the FDA. Dacarbazine or IL-2–based

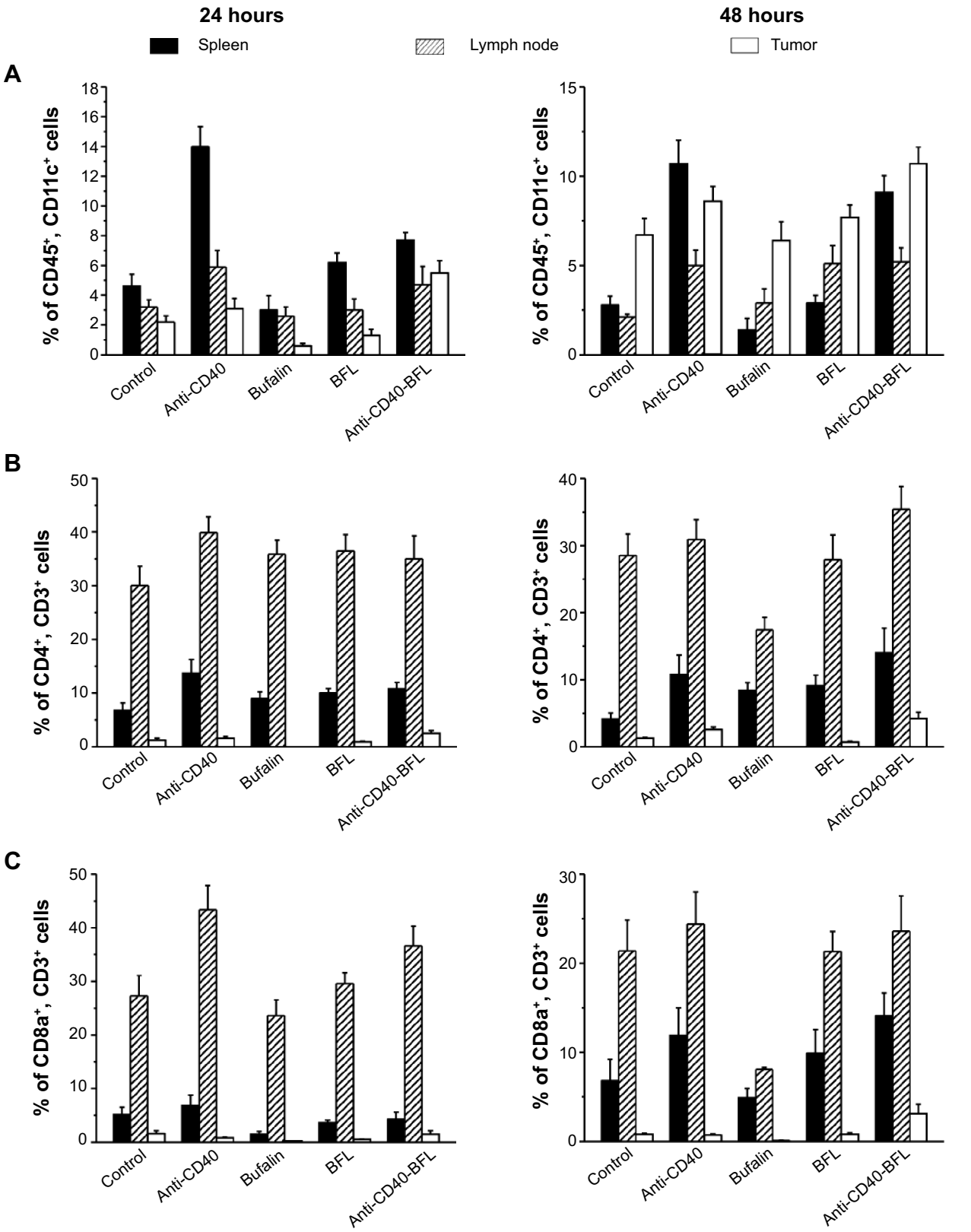

Figure 8 Bar graph summary of the flow cytometer analysis of excised tumors, spleens, and lymph nodes.

Notes: (**A**) Percentage of dendritic cells ($CD45^+CD11c^+$) in tumors, spleens, and lymph nodes after injected saline, free anti-CD40, bufalin, BFL, or anti-CD40-BFL for 24 hours or 48 hours. (**B**) Percentage of $CD4^+$ T cells ($CD3^+CD4^+$) in tumors, spleens, and lymph nodes after injected saline, free anti-CD40, bufalin, BFL, or anti-CD40-BFL for 24 hours or 48 hours. (**C**) Percentage of $CD8^+$ T cells ($CD3^+CD8a^+$) in tumors, spleens, and lymph nodes after injected saline, free anti-CD40, bufalin, BFL, or anti-CD40-BFL for 24 hours or 48 hours.

Abbreviation: BFL, bufalin liposomes.

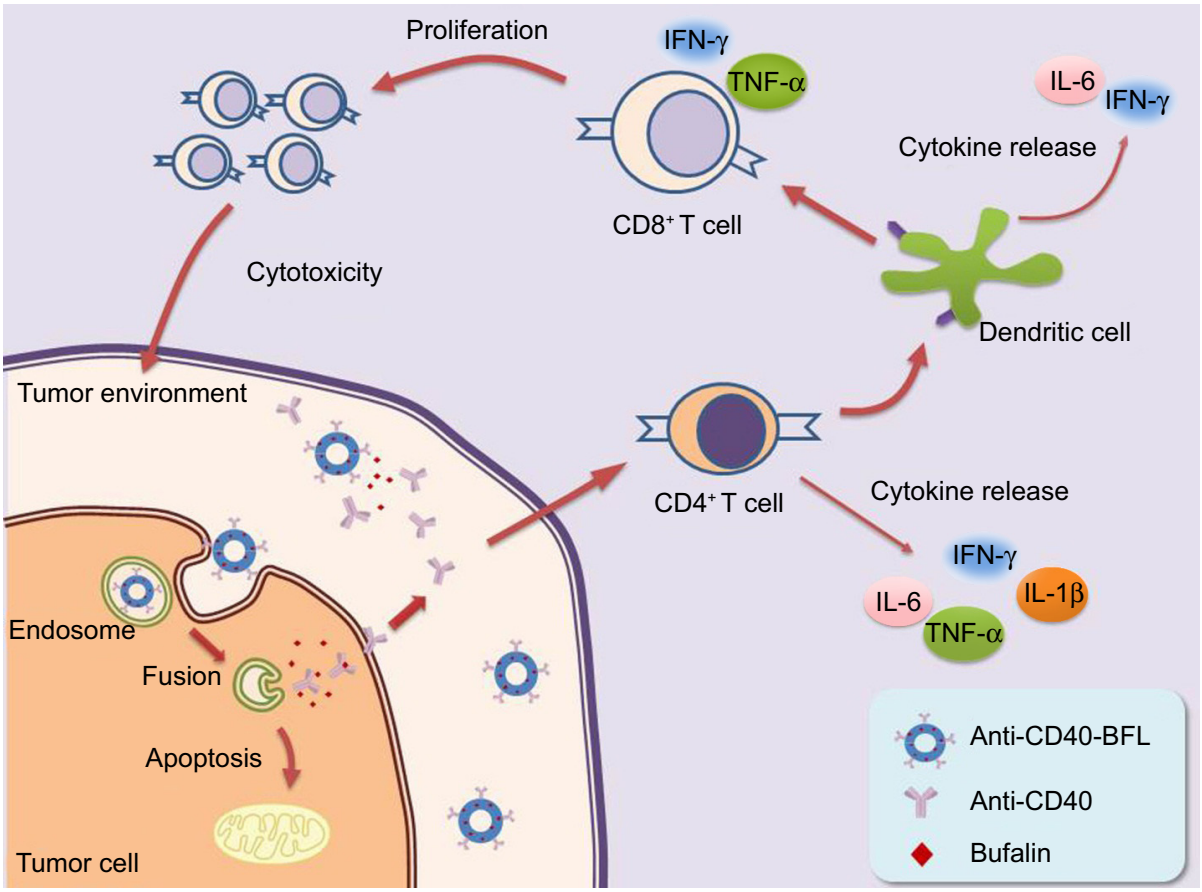

Figure 9 Schematic illustration of immunoliposome co-delivery of bufalin and anti-CD40 antibody adjuvant induce synergetic therapeutic efficacy.
Notes: After anti-CD40-BFL is injected, liposomes enter tumor cells via endocytosis. The bufalin and anti-CD40 are released after liposome fusion. Bufalin induces apoptosis via a caspase-dependent pathway. On the other hand, the anti-CD40 stimulation is delivered by CD40 ligand-expressing activated $CD4^+$ T cells. CD40 ligand binding to CD40 adhesion molecules on the surface of antigen-presenting cells, such as dendritic cells, stimulates the production of cytokines, further induces sufficient cytotoxic T lymphocytes, and produces a systemic immune response.
Abbreviations: BFL, bufalin liposome; IFN, interferon; IL, interleukin; TNF, tumor necrosis factor.

therapies are the current treatment choice; however, these have an overall modest impact on survival.[35]

Chemotherapy is the mainstay of treatment modalities for malignancies. Bufalin has been used in clinical trials for cancer treatment in China and has demonstrated induction of apoptosis in certain cancer cells. Hsiao et al[32] observed that the induction of apoptotic death in malignant melanoma A375.S2 cells by bufalin is mediated through caspase cascade-dependent and mitochondrial signaling pathways. Zhang et al[36] found that bufalin decreases the proliferation of mouse melanoma clone B16 cells with concomitant stimulation of expression of the melanotic phenotype, due to stimulation of tyrosinase activity and an increase in cellular melanin content.

Suppressive immunoreactions caused by chemotherapy drugs in the tumor microenvironment have been illustrated in the past decade,[37] and a potential therapeutic strategy to counter this immunosuppression is the use of non–cell-based therapies such as cytokines or immune receptor-targeting mAbs to break tumor-associated tolerance.[25] Massive apoptosis induced by chemotherapy can be a priming event for antitumor immunity, allowing the tumor to act as its own vaccine by releasing large amounts of tumor antigen. Immunotherapies that activate immune response pathways are of great interest for overcoming the immunosuppression present in advanced tumors. Consequently, the co-delivery strategy, with combination of chemotherapeutic drug and immune agents, has been proposed as a new strategy to achieve the synergistic effect for cancer therapies.

In this study, we choose anti-CD40 as the tumor therapy antigen for melanoma for a number of reasons. Anti-CD40 has been shown to play multiple functional roles in the immune system, including enhancing the antigen-specific T-cell response, increasing leukocyte migration, and activating macrophages.[38,39] In addition, anti-CD40 has an important effect in B-cell growth, activation of APCs including DCs,

further induction of sufficient cytotoxic T lymphocytes, and the production of a systemic immune response.

To increase the therapeutic potential of bufalin and anti-CD40, we engineered the lipid membrane bilayer comprising the liposome carriers to overcome certain limitations. The major advantages of liposomal drug delivery are: protection of active compounds from degradation; modification of drug release; an increase in circulation time; and the possibility to achieve partial site. In this study, the three most commonly used preparative methods[40] (thin-film hydration, reverse-phase evaporation, and ethanol injection) were employed to prepare liposomes composed of cholesterol, EPC, DSPE-PEG_{2000}, DSPE-PEG_{2000}-Mal, and bufalin in a molar ratio of 20:55:5:5:15, respectively. Anti-CD40 was anchored to liposome via a mild maleimide–thiol reaction. This liposome, with a size of 205.4±68.4 nm and a surface property of −15.68 mV, was able to permeate into the tumor microvasculature passively due to the permeable nature of the microvasculature in solid tumors, explained by the EPR effect. Furthermore, quantitative lipid composition of cholesterol within the liposomes was optimized to achieve the desired surface property and drug entrapment (73.59%±3.14%). The cholesterol helped to impart rigidity to the liposome system, but further enhancement above the optimized ratio leads to lipid precipitation and lower drug entrapment.[41] Modification of the surface of nanoparticles with PEG is a successful approach to prolong blood circulation time of nanoparticles, which leads to improved EPR effect-based tumor targeting of encapsulated drugs. Furthermore, the liposome formulation showed sustained release of drug in PBS. A steric protection effect endowed by the antibody chain on the surface of the liposome could minimize the drug's premature leakage, enabling accumulation of more drugs at the targeted site.

The therapeutic efficacy of anti-CD40-BFL was superior in a B16 melanoma cell mouse xenograft model, which is consistent with the results of cytotoxicity in vitro. The anti-CD40 solution had a minimal inhibitory effect in vitro, which can be explained by the absence of the CD40 receptor on the surface of B16 melanoma cells. An evident anticancer effect was induced by the active systematic immune cytotoxic T lymphocyte, which enhanced antitumor activity and was synergetic with bufalin. In addition, significant changes in body weight and cytokine levels, crucial indicators of systemic side effects, were not observed in the anti-CD40-BFL group compared with mAbs solution alone, which can be attributed to the extended release in the anti-CD40-BFL group and the avoidance of excessive systemic exposure of the liposome. The effect of anti-CD40-BFL was also stronger than bufalin, because of the ability to accumulate in solid tumors due to EPR effect and release of encapsulated bufalin inside the cells via endocytosis of the carrier.

Caspase-3, which is a common effector of most apoptotic pathways, is able to cleave several target proteins whose degradation will contribute to the execution phase of the cell-demise program.[42] Cytochrome c was the first mitochondrial protein found to participate in the mitochondria-dependent pathway.[43] In theory, caspase-3 is activated through activation of caspase-9 along with cytosolic release of cytochrome c.[44] Results from our TUNEL and Western blot assays demonstrated apoptosis in visible forms, which is consistent with our aforementioned results.

To generate lifelong immunity against tumor cells, priming of tumor-specific cytotoxic effector cells such as memory T cells is essential. Dendritic cells, one of the representative antigen-presenting cells, can present tumor antigens both on major histocompatibility complex class I and class II proteins for interaction with cytotoxic $CD8^+$ and $CD4^+$ T cells.[45] CD40-mediated stimulation of dendritic cells by $CD4^+$ T cells provides the help required by $CD8^+$ T cells. CD40 stimulation might be delivered by CD40 ligand-expressing activated $CD4^+$ T cells, which rapidly express CD40 ligand. Then CD40 ligand binding to CD40 upregulates adhesion/costimulatory molecules on the surface of APCs, such as dendritic cells, which provide the second signal required to activate naïve T cells, amplifying the immune response.[46] Immunofluorescence results indicated the combined mAbs and liposomes could be seen in the tumors, spleens, and lymph nodes after 48 hours, suggesting an extensive systemic immunity effect, as previously suspected. Compared with anti-CD40 solution, anti-CD40-BFL had higher and more enduring fluorescence intensity, which means a slow and sustained release. In addition, the number of DCs, $CD8^+$ T cells, and $CD4^+$ T cells were tested by flow cytometry to evaluate their influence on the immune system. Established B16 tumors were injected with PBS, bufalin, anti-CD40 solution, BFL, or anti-CD40-BFL. Tumor tissues, spleens, and lymph nodes were harvested 24 hours or 48 hours postinjection and processed into cell suspensions for analysis. The results indicated that the number of leukocyte cells was higher in anti-CD40 than anti-CD40-BFL groups. These results were reversed 48 hours after injection, due to the sustained-release property of liposomes. A similar change of DCs, $CD8^+$ T cells, and $CD4^+$ T cells in tumors, spleens, and lymph nodes implied an active systemic immunity effect.

Future studies will aim to elucidate the optimal proportion of antibody and chemotherapeutics in liposomal delivery.

In addition, distribution of liposome in normal tissue, such as the heart, will be of interest to further investigate the proposed reduced systemic toxicity of bufalin.

Conclusion

Here we reported the formulation and characterization of a liposomal vehicle carrying a combined dose of anti-CD40 and bufalin. This vehicle demonstrated liposome-mediated immune modulation by allowing anti-CD40 to be presented to APCs, which resulted in active potential antitumor effects. Prolonged release at the tumor site while restricting mAbs from entering systemic circulation blocks systemic toxicity. In addition, a synergistic effect of anti-CD40 with bufalin could produce enhanced antitumor responses. The results of this study provide a highly promising strategy for further investigations on other cancer types.

Acknowledgment

This work was financially supported by the National Natural Science Foundation of China (81173513) and the Natural Science Foundation of Shaanxi Province in China.

Disclosure

The authors report no conflicts of interest in this work.

References

1. Xie CM, Chan WY, Yu S, Zhao J, Cheng CH. Bufalin induces autophagy-mediated cell death in human colon cancer cells through reactive oxygen species generation and JNK activation. *Free Radic Biol Med*. 2011;51(7):1365–1375.
2. Hsu CM, Tsai Y, Wan L, Tsai FJ. Bufalin induces G2/M phase arrest and triggers autophagy via the TNF, JNK, BECN-1 and ATG8 pathway in human hepatoma cells. *Int J Oncol*. 2013;43(1):338–348.
3. Tian X, Luo Y, Yan YB, Sui CG, Meng FD, Liu YP. [Effect of bufalin on cellular proliferation and apoptosis in human esophageal squamous carcinoma EC9706 cells]. *Zhongguo Yi Xue Ke Xue Yuan Xue Bao*. 2012;34(6):556–562. Chinese.
4. Xie XB, Yin JQ, Wen LL, et al. Critical role of heat shock protein 27 in bufalin-induced apoptosis in human osteosarcomas: a proteomic-based research. *PLoS One*. 2012;7(10):e47375.
5. Pan S, Wang Y, Feng L, et al. [Study on proteomics of Hela cell apoptosis in bufalin-induced human cervical carcinoma]. *Zhongguo Zhong Yao Za Zhi*. 2012;37(13):1998–2004. Chinese.
6. Tsai SC, Lu CC, Lee CY, et al. AKT serine/threonine protein kinase modulates bufalin-triggered intrinsic pathway of apoptosis in CAL 27 human oral cancer cells. *Int J Oncol*. 2012;41(5):1683–1692.
7. Yan S, Qu X, Xu C, et al. Down-regulation of Cbl-b by bufalin results in up-regulation of DR4/DR5 and sensitization of TRAIL-induced apoptosis in breast cancer cells. *J Cancer Res Clin Oncol*. 2012;138(8):1279–1289.
8. Huang WW, Yang JS, Pai SJ, et al. Bufalin induces G(0)/G(1) phase arrest through inhibiting the levels of cyclin D, cyclin E, CDK2 and CDK4, and triggers apoptosis via mitochondrial signaling pathway in T24 human bladder cancer cells. *Mutat Res*. 2012;732(1–2):26–33.
9. Jiang Y, Zhang Y, Luan J, et al. Effects of bufalin on the proliferation of human lung cancer cells and its molecular mechanisms of action. *Cytotechnology*. 2010;62(6):573–583.
10. Li D, Qu X, Hou K, et al. PI3K/Akt is involved in bufalin-induced apoptosis in gastric cancer cells. *Anticancer Drugs*. 2009;20(1):59–64.
11. Zhang Y, Tang X, Liu X, Li F, Lin X. Simultaneous determination of three bufadienolides in rat plasma after intravenous administration of bufadienolides extract by ultra performance liquid chromatography electrospray ionization tandem mass spectrometry. *Anal Chim Acta*. 2008;610(2):224–231.
12. Qi F, Li A, Inagaki Y, et al. Antitumor activity of extracts and compounds from the skin of the toad Bufo bufo gargarizans Cantor. *Int Immunopharmacol*. 2011;11(3):342–349.
13. Nesher M, Shpolansky U, Rosen H, Lichtstein D. The digitalis-like steroid hormones: new mechanisms of action and biological significance. *Life Sci*. 2007;80(23):2093–2107.
14. Zhang HQ, Yin ZF, Sheng JY, Jiang ZQ, Wu BY, Su YH. [A comparison study of pharmacokinetics between bufalin-loaded bovine serum albumin nanoparticles and bufalin in rats]. *Zhong Xi Yi Jie He Xue Bao*. 2012;10(6):674–680. Chinese.
15. Riker AI, Sondak VK, Fishman M, Daud A, Pilon-Thomas S. Current immunotherapy of melanoma. *Clin Appl Immunol Rev*. 2005;5(2):111–132.
16. Hsueh EC, Morton DL. Antigen-based immunotherapy of melanoma: canvaxin therapeutic polyvalent cancer vaccine. *Semin Cancer Biol*. 2003;13(6):401–407.
17. Slominski A, Tobin DJ, Shibahara S, Wortsman J. Melanin pigmentation in mammalian skin and its hormonal regulation. *Physiol Rev*. 2004;84(4):1155–1228.
18. Slominski AT, Carlson JA. Melanoma resistance: a bright future for academicians and a challenge for patient advocates. *Mayo Clin Proc*. 2014;89(4):429–433.
19. Kiran KL, Lakshminarayanan S. Optimization of chemotherapy and immunotherapy: in silico analysis using pharmacokinetic–pharmacodynamic and tumor growth models. *J Process Control*. 2013;23(3):396–403.
20. Alderson KL, Luangrath M, Elsenheimer MM, et al. Enhancement of the anti-melanoma response of Hu14.18K322A by αCD40 + CpG. *Cancer Immunol Immunother*. 2013;62(4):665–675.
21. Frazier JL, Han JE, Lim M, Olivi A. Immunotherapy combined with chemotherapy in the treatment of tumors. *Neurosurg Clin N Am*. 2010;21(1):187–194.
22. Khalil M, Vonderheide RH. Anti-CD40 agonist antibodies: preclinical and clinical experience. *Update Cancer Ther*. 2007;2(2):61–65.
23. Zhang B, Wu T, Chen M, Zhou Y, Yi D, Guo R. The CD40/CD40L system: a new therapeutic target for disease. *Immunol Lett*. 2013;153(1–2):58–61.
24. Qu X, Felder MAR, Perez Horta Z, Sondel PM, Rakhmilevich AL. Antitumor effects of anti-CD40/CpG immunotherapy combined with gemcitabine or 5-fluorouracil chemotherapy in the B16 melanoma model. *Int Immunopharmacol*. 2013;17(4):1141–1147.
25. Kwong B, Liu H, Irvine DJ. Induction of potent anti-tumor responses while eliminating systemic side effects via liposome-anchored combinatorial immunotherapy. *Biomaterials*. 2011;32(22):5134–5147.
26. Luo LM, Huang Y, Zhao BX, et al. Anti-tumor and anti-angiogenic effect of metronomic cyclic NGR-modified liposomes containing paclitaxel. *Biomaterials*. 2013;34(4):1102–1114.
27. Li F, Weng Y, Wang L, He H, Yang J, Tang X. The efficacy and safety of bufadienolides-loaded nanostructured lipid carriers. *Int J Pharm*. 2010;393(1–2):203–211.
28. Iyer AK, Su Y, Feng J, et al. The effect of internalizing human single chain antibody fragment on liposome targeting to epithelioid and sarcomatoid mesothelioma. *Biomaterials*. 2011;32(10):2605–2613.
29. Gao JQ, Lv Q, Li LM, et al. Glioma targeting and blood–brain barrier penetration by dual-targeting doxorubincin liposomes. *Biomaterials*. 2013;34(22):5628–5639.
30. Arranz A, Reinsch C, Papadakis KA, et al. Treatment of experimental murine colitis with CD40 antisense oligonucleotides delivered in amphoteric liposomes. *J Control Release*. 2013;165(3):163–172.

31. Broos S, Sandin LC, Apel J, et al. Synergistic augmentation of CD40-mediated activation of antigen-presenting cells by amphiphilic poly(γ-glutamic acid) nanoparticles. *Biomaterials*. 2012;33(26):6230–6239.
32. Hsiao YP, Yu CS, Yu CC, et al. Triggering apoptotic death of human malignant melanoma a375.s2 cells by bufalin: involvement of caspase cascade-dependent and independent mitochondrial signaling pathways. *Evid Based Complement Alternat Med*. 2012;2012:591241.
33. Jinturkar KA, Anish C, Kumar MK, Bagchi T, Panda AK, Misra AR. Liposomal formulations of etoposide and docetaxel for p53 mediated enhanced cytotoxicity in lung cancer cell lines. *Biomaterials*. 2012;33(8):2492–2507.
34. Sanki A, Scolyer RA, Thompson JF. Surgery for melanoma metastases of the gastrointestinal tract: indications and results. *Eur J Surg Oncol*. 2009;35(3):313–319.
35. Mittendorf EA, Lim SJ, Schacherer CW, et al. Melanoma adrenal metastasis: natural history and surgical management. *Am J Surg*. 2008;195(3):363–368; discussion 368–369.
36. Zhang L, Yoshida T, Kuroiwa Y. Stimulation of melanin synthesis of B16-F10 mouse melanoma cells by bufalin. *Life Sci*. 1992;51(1):17–24.
37. Nowak AK, Robinson BW, Lake RA. Synergy between chemotherapy and immunotherapy in the treatment of established murine solid tumors. *Cancer Res*. 2003;63(15):4490–4496.
38. Xie F, Shi Q, Wang Q, et al. CD40 is a regulator for vascular endothelial growth factor in the tumor microenvironment of glioma. *J Neuroimmunol*. 2010;222(1–2):62–69.
39. Eliopoulos AG, Young LS. The role of the CD40 pathway in the pathogenesis and treatment of cancer. *Curr Opin Pharmacol*. 2004;4(4):360–367.
40. Yang S, Chen J, Zhao D, Han D, Chen X. Comparative study on preparative methods of DC-Chol/DOPE liposomes and formulation optimization by determining encapsulation efficiency. *Int J Pharm*. 2012;434(1–2):155–160.
41. Abreu AS, Castanheira EM, Queiroz MJ, Ferreira PM, Vale-Silva LA, Pinto E. Nanoliposomes for encapsulation and delivery of the potential antitumoral methyl 6-methoxy-3-(4-methoxyphenyl)-1H-indole-2-carboxylate. *Nanoscale Res Lett*. 2011;6(1):482.
42. Nestal de Moraes G, Carvalho É, Maia RC, Sternberg C. Immunodetection of caspase-3 by Western blot using glutaraldehyde. *Anal Biochem*. 2011;415(2):203–205.
43. Giegé P, Grienenberger JM, Bonnard G. Cytochrome c biogenesis in mitochondria. *Mitochondrion*. 2008;8(1):61–73.
44. Nagase M, Shiota T, Tsushima A, et al. Molecular mechanism of satratoxin-induced apoptosis in HL-60 cells: activation of caspase-8 and caspase-9 is involved in activation of caspase-3. *Immunol Lett*. 2002;84(1):23–27.
45. Paulis LE, Mandal S, Kreutz M, Figdor CG. Dendritic cell-based nanovaccines for cancer immunotherapy. *Curr Opin Immunol*. 2013;25(3):389–395.
46. Costello RT, Gastaut JA, Olive D. What is the real role of CD40 in cancer immunotherapy? *Immunol Today*. 1999;20(11):488–493.

Supplementary materials

Table S1 Characterization of BFL and anti-CD40-BFL

Liposome formulation	Particle size (nm), mean ± SD	Polydispersity	Zeta potentials (mV)
BFL	171.4±69.2	0.088	−30.71
anti-CD40-BFL	205.4±68.4	0.062	−15.68

Abbreviations: BFL, bufalin liposomes; SD, standard deviation.

Table S2 Cytotoxicity of bufalin and liposomal formation against B16 cells (n=6)

Bufalin formulation	IC_{50} (nmol/mL)	SD
Bufalin	224.12	3.14
BFL	69.91	0.93
Anti-CD40-BFL	61.73	1.21

Abbreviations: BFL, bufalin liposomes; IC_{50}, 50% inhibitive concentration; SD, standard deviation.